ISSN 0101-2061 (Print)
ISSN 1678-457X (Online)

DOI: https://doi.org/10.1590/fst.02618

Optimizing the texture and retrogradation properties of Niangao (Rice Cake) made with naturally fermented rice flour

Nianjie FENG[1], Shimiao TANG[1,2], Mengzhou ZHOU[1,2], Zhejuan LV[3], Yuanyuan CHEN[1,2], Panheng LI[1,2], and Qian WU[1,2*]

Abstract

Niangao is prepared from polished round-grained or waxy rice flour and it is a popular and traditional steamed rice cake in China, but its preparation is different. In this study, *Niangao* was produced with naturally fermented rice flour and the effects of fermentation on physical properties and rheological characteristics were investigated. The results suggest that the water-holding capacity, texture, and color of the samples were significantly improved after natural fermentation, while amylose content was decreased. Additionally, fermentation had a marked effect on retarding the retrogradation of *Niangao* because fermented *Niangao* exhibited lower degree of retrogradation compared with the control. Control means *Niangao* which was produced by unfermented rice flour. Fermented *Niangao* was harder to be digested than the control was.

Keywords: fermentation; *Niangao* (rice cake); retrogradation.

Pratica Application: Fermentation of *Niangao* resulted in the improvement of sensorial taste.

1 Introduction

Rice is one of the major food crops worldwide, and more than 50% of the world's population depends on rice as the primary caloric source (Zhang et al., 2010). Rice products are staple foods, especially in China, who is the world's largest rice producer and consumer. Rice products have many unique attributes, such as ease of digestion, bland taste, and hypoallergenic properties (Roman et al., 2017). Various kinds of instant foods and fresh-cooked rice products, such as cooked rice grains, rice noodles, infant rice foods, baking rice goods, and beer or wine, share the market (Wang et al., 2018). *Niangao* (rice cake) is a popular traditional food in China, and this food has been served at festivals and feasts for the past 2000 years. This rice cake is different from steamed sponge cake (Fagao) in China in terms of its production, mouth feel, texture, flavor, and features (such as water content, appearance, microstructural aspects, and rheological properties). During storage, the high retrogradation rate of starch leads to a shortened shelf life of *Niangao*. Undesirable characteristics, such as moisture loss, flavor loss, increased firmness, and poor viscosity could occur. Therefore, improving the stability of *Niangao* would contribute to extending its shelf-life and higher market promotion.

Many countries use natural fermentation as a common traditional process to treat grain. The taste, mouth feel, and flavor of produced rice improve after natural fermentation of whole rice grains, and safety and nutrition of products are also enhanced (Zhu, 2018). Many types of fermented food from grain, such as the Mexico's pozol (Falguni et al., 2011), Turkey's Boza (Kancabaş & Karakaya, 2013), and India's chapatti (Sharma et al., 2017), are available worldwide. Fermented cassava starch has better extrusion properties, which could be beneficial to improve bread quality. Studies have shown that fermented rice food contains many functional constituents, such as amino acids, functional oligosaccharide, antioxidant activity substances (e.g., VitB12, nucleotide and aromatic compounds). Fermented rice food also contains other functional compounds which can reduce cholesterol and blood pressure. Examples of these compounds are gaba (gamma-GA-BA) and some peptides, which can inhibit the serum lipid peroxidation, reduce blood cholesterol content, and enhance the antithrombotic function in the human body. Moreover, fermented food produces some beneficial microbes, such as lactic acid bacteria, and enzymes, such as protease, amylase, and digestive enzymes (Zhou et al., 2017).

Natural fermentation mainly occurs in the starch amorphous area, in which changes in the structure and composition of amylopectin are observed. Fermented rice flour more easily forms a clear and transparent paste than the control due to starch degradation caused by microorganism fermentation (Lu et al., 2005). Fermentation has a certain degree of impact on the characteristics of rice starch particles. For instance, the particle sizes of starch are reduced and became consistent with grain sizes. This characteristic can be beneficial to form a uniform gel and make a starch grain surface acquire a kraurotic-like erosion mark. Fermentation can also change the crystallinity of starch but not its crystal form (Somsubsin et al., 2018).

Received 15 Mar., 2018
Accepted 29 Sept., 2018
[1] *Hubei University of Technology, Wuhan, Hubei 430068, China*
[2] *Key Laboratory of Fermentation Engineering, Hubei Key Laboratory of Industrial Microbiology, Hubei Provincial Cooperative Innovation Center of Industrial Fermentation, Wuhan, Hubei 430068, China*
[3] *College of Food Science and Technology, Huazhong Agricultural University, Wuhan, Hubei 430070, China*
*Corresponding author: qianwill2007@163.com

The gelatinisation of rice and structural characteristics of rice products are significantly related. Fermentation has significantly influence on pasting temperature, peak sticky degree, minimum viscosity, final viscosity, collapse value, and retrogradation value of rice flour. The retrogradation value of rice flour is notably reduces after fermentation, which may cause a reduction in the short-term staling ability (Yang & Tao, 2008). Starch recrystallization will also be hindered in an acidic environment after fermentation (Xiong et al., 2010).

Increase in amylose content and production of lactic acid contribute to the formation of a gel network and increase in gel strength. At the same time, after fermentation the gel exhibits better aging resistance properties because of the decrease in the heavy crystallization ability of amylopectin. Fermentation considerably changes the physicochemical properties of rice flour. Thus, the quality and functional properties, taste, and flavor of rice products are also obviously improved. However, the characteristics of *Niangao*, especially that of fermented *Niangao*, has not been reported yet. In China, the traditional *Niangao* production has become industrialized and the technology is increasingly mature. But the digestion rate of traditional *Niangao* is not very high, and it is in short in storage period and easy to deteriorate, that make the market popularity of traditional *Niangao* relatively low. In this study, the effects of natural fermentation on the structure, texture, whiteness, water-holding capacity (WHC) and retrogradation rate of *Niangao* were investigated to improve the properties and extend the shelf life of this food.

2 Materials and methods

2.1 Materials

Waxy rice and polished round-grained rice were purchased from Tianyuan Biotechnology Company (Hanchuan, HuBei, China). Moisture (method 44-15A), protein (method 46-11A), ash (method 08-01), and lipid (method 30-10) contents of the rice flours were measured according to the methods defined by the American Association of Cereal Chemist (2000). All other chemicals used were of analytical grade, and distilled water was used in the experiment.

2.2 Preparation of Niangao

The ingredients (40 g of polished round-grained rice, 20 g of waxy rice, 180 mL of water) were mixed, sealed, and incubated at 25 °C for 2 days (natural fermentation). The fermented rice was ground into thick liquid using a ball grinder (JP-DM, China). Then, the rice slurry was quickly leached for 40 min to remove the water using a vacuum suction filter pump. The dry rice flour (moisture content of 40%) obtained from leaching was sieved through a 20 mesh screen, shaped by a mold, and then steamed for 10 min in an electric cooker preheated to 100 °C. Then, after kneading and cooled at room temperature, the *Niangao* samples were packaged in polyethylene bags and then cut into pieces ($35\times25\times1.2$ mm^3). The sample made of rice soaked for only 4 h was referred to as control. A photo of *Niangao* is shown in Figure 1.

Figure 1. Appearance of freshly sliced *Niangao.*

2.3 Analysis of amylose content

The amylose content of the rice flour starch in *Niangao* was determined by the method of Juliano with slight modifications (Juliano et al., 2012). The sample (100 mg) was dispersed in 1 mL of 95% ethanol and 9 mL of 1 mol/L NaOH. The flour slurry was heated for 10 min in a boiling water bath to gelatinize the starch. The starch solution was mixed with 1 mL of 1 mol/L acetic acid and 2 mL of iodine solution (0.2 g of iodine and 2.0 g of potassium iodide in 100 mL of aqueous solution). The mixture was stirred well and allowed to stand for 20 min. Absorbance was then measured at 620 nm using a WFZ UV2100 spectrophotometer (UNICO, Shanghai).

2.4 Color measurement

The surface reflectance of the fermented *Niangao* and control (samples were under a plate glass with a thickness of 1.2 mm) was measured using the UltraScan XE measuring color difference meter, model RSIN (Hunter Associates Laboratory, Reston, VA, USA). The instrument was calibrated against a standard white reference tile (X=93.60, Y=91.60, Z=109.70). Hunter L (lightness), a (redness), and b (yellowness) values were obtained using the setting of D65 (daylight, 65 light angle). The average value from three random locations on the surface of each sample was used for statistical analysis. The whiteness (W) was calculated as follows (equation 1):

$$W = 100 - \sqrt{(100-L)^2 + a^2 + b^2} \quad (1)$$

2.5 Water-holding capacity

WHC was determined using a published method with additional modifications (Hoove & Vasanthan, 1993). Dry sample (0.5 g) was weighed precisely into a test tube (vol. 7 mL), and 5 mL of distilled water added. The formation of lumps was prevented by mixing in a Vortex mixer at room temperature for 20 min and then centrifuging at 2500 rpm for 5 min (TGL-16C, Shanghai Anting Science Instrument Co.). The supernatant and residue were separated, and the residue was weighed. The quantity of dry matter in the supernatant was determined by drying at 105 °C, until a constant weight was obtained. WHC was calculated as follows: $WHC = \frac{G}{0.5 - G1} \times 100\%$, where G is the mass of residue in the test tube forming part of the dry matter, and G1 is the mass of dry matter in the supernatant forming another part of the dry matter.

2.6 Texture and sensory property

A textural analyzer (TA-XT$_2$, Stable Microsystems Ltd, Surrey, UK) was used to evaluate instrumental the sample texture. Sample (15×15×12 mm^3) were prepared using a stainless frame device and then placed on the platform. A cylinder-type stainless steel probe with a diameter of 50 mm was used to compress each sample to 50% of its original height with pre-test speed of 2.0 mm/s, test speed of 1.0 mm/s, and post-test speed of 1.0 mm/s. The average of at least 10 replicates was considered (Seo et al., 2007). The sensory evaluation test for *Niangao* was performed by trained panelists using a 9-point test. The evaluated attributes were color, off-flavor, delicate taste, sweetness, smoothness, softness, adhesiveness, and moistness for the difference test, and overall quality for the preference test.

2.7 X-Ray Diffraction (XRD)

To evaluate the recrystallization of the retrograded *Niangao*, the crystalline characteristics of fresh and retrograded *Niangao* were analyzed with a D/max-RAIII X-ray diffractometer equipped with a copper tube operating at 35 kV and 30 mA, producing CuKα radiation of 0.154 nm wavelength. Diffractograms were achieved by scanning from 3° to 50° (2θ) at a rate of 8° /min, step size of 0.02°, divergence slit width of 1°, receiving slit width of 0.02 mm, and scatter slit width of 1°. The staling *Niangao* samples were stored at 4 °C for 5 days, dried at 35 °C for 24 h, and subsequently ground into powder before analysis.

All analyses were conducted in triplicate, and MDI Jade 5.0 evaluation of integrals was used to calculate the diffractograms. The crystallinity of the samples can be quantified by integrating the area under the fitting crystalline peaks. The software JADE 5.0 was used to deduct deduct the amorphous bottom, smoothing, and fitting the original peak to obtained the integrated areas. The relative crystallinity (X_{RC}) was indicated as $X_{RC}=(Is/Ic)\times 100$, where Is is the integrated area of crystalline peaks in the treated samples, and Ic is the integrated area of the total strength of the diffraction peak (Primo-Martin et al., 2007).

2.8 Differential Scanning Calorimetry (DSC)

The retrogradation properties of *Niangao* samples were analyzed by a differential scanning calorimeter (DSC204F, NETZSCH, German) using stainless steel pans (PE 0319-0218). The equipment was calibrated with indium and tin standard, and an empty pan was used as a reference. Weighed samples (5 mg) removed from the central portion of the *Niangao* were hermetically sealed in aluminum to avoid moisture loss. Duplicate sample pans were prepared and each sample was heated from 20 °C to 150 °C at 5 °C/min. The temperature values obtained were the difference of the onset temperatures of transition (To) and the temperatures at the completion of transition (Tc). The peak transition temperature (Tp) was defined as the temperature at the maximum peak. The enthalpy of transition was estimated from the integrated heat flow over the temperature range of the transition, and is expressed as joule per gram of sample (J/g) (Irondi et al., 2017).

2.9 Scanning Electron Microscopy (SEM)

The structural properties of the microprofiles caused by the changes in retrogradation for *Niangao* were studied using a scanning electron microscope (HITACHI X-650, NTC company, Japan). All the samples were cut into pieces with thickness of approximately 1 cm and slice area of 4 cm^2 and then dried at 35 °C for 24 h before tests. The samples were positioned on an aluminum bar using a double-sided stick tape and were plated with a thin film of gold-palladium (60:40) onto the surface. The samples were examined at an accelerating voltage of 10 kV. Image J 1.42 q and plugin of FracLac -2.5. Release 1 d were used to analyze the scanning electron micrograph with binarization processing (Dàvila & Parés, 2007).

2.10 Digestion of starch in vitro

A 0.5 g portion of the sample was mixed with 25 mL of phosphate buffer (pH 6.9) and 5 mL of phosphate buffer which contained 2.6 units of α-amylase (A3176, Sigma). The flour slurry was placed in constant temperature water bath at 37 °C and oscillated. Then, 1 mL of the sample was taken out every 30 min for 3.5 h and heated in a boiling water bath and oscillated for 5 min to inactivate the enzyme. Then, the solution was cooled to room temperature. The sample (1mL) was mixed with 3 mL of 0.4 mol/L sodium acetate buffer (pH 4.75) and 20 μL of glucosidase (A3042, Sigma). Then, the mixture was oscillated under constant temperature at 55 °C for 45 min to hydrolyze starch to glucose. Glucose content was determined by DNS method. Starch content was determined by multiplying glucose content by the conversion factor (0.9), and each sample was measured in three parallel measurements.

2.11 Statistical analysis

All statistical analyses were performed using Origin software 8.0. Data were presented as means±standard deviation (SD) and calculated using one-way ANOVA of SPSS 17.0, followed by Tukey's multiple-range test. Statistical significance was defined as $p< 0.05$ or $p< 0.01$.

3 Results and discussion

3.1 Composition and physical properties

The approximate compositions of the raw materials are listed in Table 1. The physical properties and color values of fermented and control samples are shown in Table 2. The apparent amylose content in the fermented *Niangao* was evidently lower ($p<0.01$) than in the control. This phenomenon was probably due to the fact that organic acid, glucoamylase and alpha-amylase were generated during fermentation and the amorphous area of the starch granule was hydrolyzed. This event apparently reduced the soluble amylose content, which was in accordance with other reports (Alonso-Gomez et al., 2016). In addition, most of the amylose fraction was quickly degraded by acid and enzymes at the start of hydrolysis (Franco et al., 2002). *Niangao* with lower amylose content may have chewy texture and lower retrogradation rate, which would significantly delay the stalling of starch during storage at low temperature. During storage, the retrogradation of starch was partly affected by amylose chain reassociation (Auh et al., 2006). The amylopectin content of fermented *Niangao* was increased by 4.79% comparing with that of the unfermented *Niangao*. After fermentation, the recrystallization ability of the starch gel decreased during storage, resulting in good ageing resistance ability (Xiong et al., 2010). Conversely, a significant difference in WHC was found between the fermented and control ($p<0.01$). The WHC of the fermented sample was higher than that of the control. This characteristic may be due to the dissolution of some short-branched amylopectin during natural fermentation. This result was consistent with those studies in which the short-chain amylopectin with 5-9 glucose units was inferred to increase the swelling capacity (Jiang et al., 2013; Vandeputte et al., 2003). The change in the structure and composition of rice starch greatly influenced the quality of products after fermentation. The taste of *Niangao* was apparently more exquisite, and its structure was more elastic.

The lightness (L), redness (+a), and yellowness (+b) of the two kinds of *Niangao* differed notably ($p<0.05$). Overall, fermentation improved the whiteness of *Niangao* ($P<0.01$) (Table 2), which can be ascribe to starch purification and the decrease in crude lipids and ash content after fermentation (Park et al., 2012). This phenomenon may be due to the fact that rice protein and fat were degraded by microbial fermentation, and the mineral elements, which were embedded by the combination of protein, fat, and starch, were released and were more easily dissolved (Xie et al., 2017). Thus, the ash content of samples decreased, and the fermented *Niangao* appeared whiter and more transparent compared with the unfermented control *Niangao*.

Table 1. Proximate composition of raw materials.

Materials	Properties			
	Protein (%)	Crude lipid (%)	Total ash (%)	Moisture (%)
Waxy rice	7.34±0.08	0.87±0.07	0.51±0.12	14.08±0.11
Polished round-grained rice	6.54±0.15	0.98±0.10	0.59±0.11	15.30±0.07

Means (three replicates); ±Standard Deviation.

Table 2. The physical properties of fermented and control *Niangao*.

Properties	*Niangao*	
	Control	Fermented
Amylose content (%)	26.36±0.15	18.42±0.33**
Amylopectin content (%)	23.27±0.18	28.06±0.23**
Protein content (%)	6.57±0.10	6.32±0.09*
Crude lipid content (%)	0.59±0.06	0.54±0.02
Total ash content (%)	0.46±0.02	0.39±0.02*
Water-holding capacity (%)	96.87±1.03	115.09±1.11**
Color value, L	68.61±0.22	70.61±0.37**
a	−1.55±0.07	−1.19±0.12*
b	3.42±0.29	1.94±0.13**
Whiteness (%)	69.41±0.19	71.52±0.21**

Means (three replicate) ±Standard Deviation; **, $p<0.01$ versus control; *, $p<0.05$ versus control.

3.2 Textural and sensory properties

The textural and sensory properties of *Niangao* are listed in Table 3. Hardness, adhesiveness, cohesiveness, and chewiness significantly differed ($p<0.05$). The chewiness and hardness of fermented *Niangao* were significantly higher than those of control ($p<0.01$). This phenomenon suggested that the fermented samples may be slightly firmer compared with the unfermented one. Moreover, evident increase in adhesiveness and cohesiveness were observed after fermentation ($p<0.05$). Adhesiveness was increasehad and depended on the combined effect of adhesive and cohesive forces, as well as the viscosity and viscoelasticity (Qi & Sun, 2010).

The trained panelists evaluated two kinds of *Niangao*, which had been freshly prepared (Table 3). The color, smoothness, and moistness of fermented *Niangao* scored higher than those of unfermented one ($p<0.05$). Although no obvious difference was found in softness, the overall quality of the fermented sample received a higher score. After fermentation, the reduced fat and protein contents of rice flours resulted in the release of starch grains which were originally combined. Simultaneously, the intramolecular and intermolecular in rice starch formed hydrogen bonds and an ordered network structure. Thus, fermented *Niangao* showed favorable chewy and flexible taste (Carmona-García et al., 2016).

3.3 X-Ray Diffraction analysis (XRD)

Final recrystallization was investigated by XRD to prove the effect of fermentation on retarding the retrogradation of *Niangao*. XRD patterns and corresponding crystallinity which

Table 3. Textural and sensory properties of fermented and control *Niangao*.

Properties	*Niangao*	
	Control	Fermented
Textural properties		
Hardness	1059.37±103.30	1476.15±89.00**
Adhesiveness	200.59±28.50	319.93±23.30**
Cohesiveness	0.84±0.10	0.94±0.11*
Chewiness	682.08±0.08	1055.72±0.09**
Springiness	0.25±0.07	0.25±0.07
Resilience	0.75±0.33	0.76±0.13
Sensory properties		
Color	7.24±0.76	8.14±0.95*
Softness	7.32±0.98	7.30±0.95
Smoothness	6.15±1.12	7.25±1.20*
Moistness	6.24±0.85	7.85±0.91**
Overall quality	6.54±0.55	7.55±0.64**

Means(three replicate), ±Standard Deviation; **, $p<0.01$ versus control; *, $p<0.05$ versus control. Overall quality was evaluated by preference test, and other attributes were accomplished by a different test from weak (1) to strong (9) points.

were observed from fermented and unfermented *Niangao* flour, are shown in Table 4.

Anabiosis is a straight part of amylose and amylopectin which showed a linear array, that is, from amorphous form reverting back to crystals. This parallel arrangement is a direct internal driving force of series of stalling phenomenon (Wu et al., 2010). The retrograded starch provided several peaks at approximately 2θ angles of 17°, 20°, and others (Niu et al., 2018), which were typical patterns of retrograded starch (B-type), and the pattern was clearly distinct from that of raw starch. This phenomenon was accompanied by a gradual increase in rigidity and phase separation between the polymer and the solvent (syneresis). B-type crystallinity was characterized by a well-defined peak at 17° (2θ). The formation of this peak was the result of the crystallization of melting amorphous starch, which was mainly caused by increased amylopectin fraction during storage (Thiré et al., 2003; Osella et al., 2005). The peak at 20° corresponded to the presence of crystalline V-type amylose–lipid complexes formed during processing (Romano et al., 2018).

Two major broad peaks were identified in all retrogradated *Niangao* samples at 2θ angles at nearby 24° and 39° (Figure 2). The intensity of the diffraction peaks of retrograded fermented *Niangao* was apparently lower than that of the control (Figure 2).

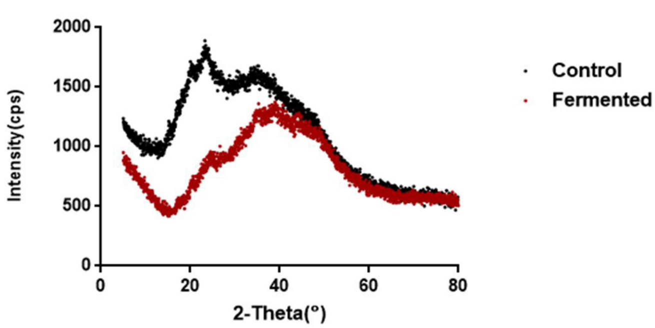

Figure 2. X-diffraction spectra of fermented and control *Niangao*.

Table 4. Relative crystallinity (X_{RC}) in retrograded samples as determined using x-ray diffraction.

Niangao	X_{RC} %
Control	100
Fermented	72.90±4.78

Means (three replicate) ± Standard Deviation (*n*=3). X_{RC}, which is the relative crystallinity, was calculated as follows: $X_{RC}=(Is/Ic)\times100$, where *Is* is the integrated area of fitting crystalline peaks (24° and 39°) in the treated samples, and *Ic* is the integrated area of fitting crystalline peaks (24° and 37°) in the control. Relative crystallinity of the control is 100.

Given that the XRD peak of the retrograded starch was normally the dispersive broad peak (Seo et al., 2007; Niu et al., 2018), we used MDI Jade 5.0 software to smooth and fit these peaks to calculate crystallinity. Two peaks at 24° and 37° were found for the control *Niangao*, while two peaks at 24° and 39° were found for fermented *Niangao* in each original pattern. Therefore, crystallinity was quantified by integrating the area under the fitting crystalline peaks. The relative crystallinity of fermented *Niangao* was markedly decreased to 72.90% compared with that of the control (100%). Both *Niangao* samples had strong diffraction peaks at 24°, and these peaks were characteristic diffraction peaks of B-type crystallization. The fermented *Niangao* had a small swelling peak at 24°, but the peak intensity of this position was much lower than that of control *Niangao*. These results implied that fermentation could retard the recrystallization or retrogradation behavior of rice flour in *Niangao*. These observations agreed with the following results on retrogradation endotherm value in DSC.

3.4 Thermal analysis

The enthalpy values of retrograded starch reflect the melting of the crystallites, which were formed by association between adjacent double helices during gel storage (Santiago-Ramos et al., 2018). This endotherm peak was due to the melting of retrograded amylopectin (Gunaratne et al., 2011) rather than amylose. The degree of starch retrogradation was measured using the enthalpy values (△H) of the endothermic peak from 40 °C to 60 °C in the DSC thermograms. This peak was characteristic of the melting of retrogradated amylopectin. Table 5 lists the retrogradation transition temperature (*T*o, *T*p, and *T*c) and △H of samples after 5 days of storage at 4 °C and 16 days of storage at -18 °C. Fermented *Niangao* had lower △H compared with the control at 4 °C and -18 °C. The results revealed that fermentation effectively inhibited starch retrogradation in *Niangao*. For both kinds of *Niangao*, the increase in the values of △H at 4°C storage condition was greater than that those at -18 °C storage. Compared with those at -18 °C storage, the retrogradation of *Niangao* at 4 °C storage was more rapid. This phenomenon may be due to the fact that the protein and lipid contents of rice flour markedly decreased after fermentation such that starch, which was originally combined with protein or lipid, was released during fermentation, thereby purifying the rice starch (Lu et al., 2003). Compared with the known hydrophilicity of wheat gluten, lipids and rice proteins are hydrophobic (Peng et al., 2017). These modifications made rice starch acquire higher WHC to prevent starch molecular recrystallization during storage.

Table 5. Retrogradation temperatures and enthalpy of gelatinized *Niangao* after 5 days' storage at 4 °C and 16 days' storage at -18 °C.

	Niangao	*T*o (°C)	*T*p (°C)	*T*c (°C)	△H (J/g)
5 days of storage at 4 °C	Control	43.8±0.3	48.1±0.5	54.0±0.8	1.65±0.06
	Fermented	40.8±0.4	43.5±0.3	48.6±0.5	0.62±0.04**
16 days of storage at -18 °C	Control	43.3±0.5	47.1±0.3	53.8±0.9	1.34±0.11
	Fermented	42.8±0.7	44.9±0.2	49.4±0.4	0.83±0.08**

Means(three replicate)± Standard Deviation; **, $p<0.01$ versus control. *T*o, onset temperature; *T*p, peak temperature; *T*c, conclusion temperature; △H, enthalpy of retrogradation.

3.5 Morphological properties

The scanning electron micrographs of the texture profile of the fermented and control *Niangao* samples at magnifications of 300×100 μm and 500×100 μm are illustrated in Figure 3 and listed in Table 6. The texture of fermented and control *Niangao* exhibited significant variations in shape. Although these surfaces appeared to have a honeycomb-like structure, which may be due to the high loss of water during storage, the fermented sample apparently had smoother and more intact structure than unfermented samples (Figure 3). Therefore, the microstructure could be used as the evaluation index to distinguish fresh from retrograded *Niangao*.

Fractal dimension reflects the complexity of a system. Fractal dimension becomes higher when a system is more complex. This characteristic shows the complexity of the curve, and the trends of filling with the scope of the plane (Xie et al., 2017). For *Niangao*, the higher fractal dimension was, the more incomplete the internal structure was, and the finer particles were. The pore equivalent diameter is inversely proportional to the fractal dimension. The smaller the pore equivalent diameter is, the smaller the inner structure particle is and the whole plane tended to be filled. Table 6 shows that the unfermented *Niangao* had higher fractal dimension and lower average pore equivalent diameter compared with the fermented *Niangao*. The structure of the control was evidently more compact, indicating the higher crystallinity of the structure and higher retrogradation.

3.6 Digestion rate of starch

The digestion rates of starch in fermented and control *Niangao* are shown in Figure 4. The digestion rate of starch in fermented *Niangao* was faster than that of control *Niangao* with time. The hydrolysis reached balance after 3 hours. This phenomenon illustrated that fermented *Niangao* was more digestible than control *Niangao* and the nutrients of the former were more easily absorbed by people.

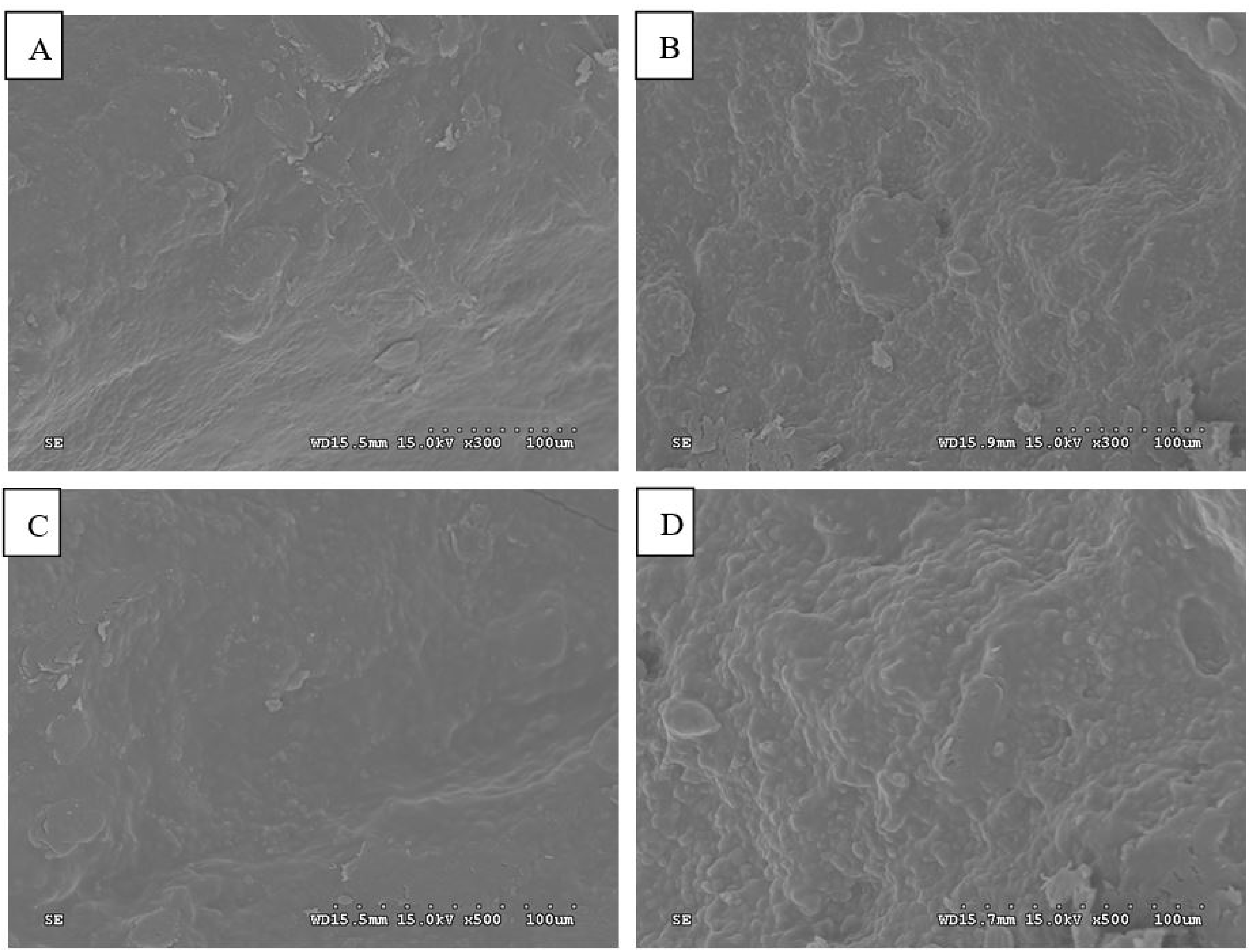

Figure 3. Scanning electron micrographs of *Niangao*. (A) Fermented *Niangao* at magnification of 300×100 μm. (B) Control *Niangao* at magnification of 300×100 μm. (C) Fermented *Niangao* at magnification of 500×100 μm. (D) Control *Niangao* at magnification of 500×100 μm.

Table 6. The pore equivalent diameter and fractal dimension of the SEM of *Niangao* samples.

Time–temperature	Pore equivalent diameter		Fractal dimension	
	Fermented	Control	Fermented	Control
Fresh	0.384±0.012	0.236±0.008**	0.041±0.004	0.044±0.002
5 days of storage at 4 °C	0.329±0.008	0.243±0.011**	0.043±0.002	0.046±0.003

Means (three replicate)± Standard Deviation; **, p<0.01 versus control.

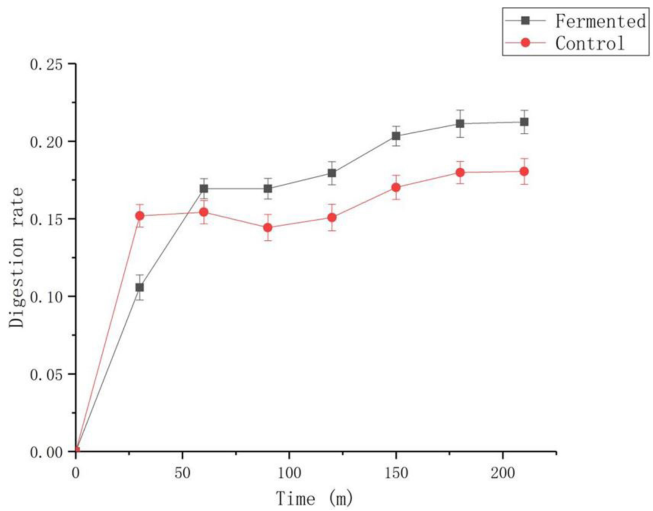

Figure 4. Digestion rate of fermented and control *Niangao*.

4 Conclusions

Natural fermentation of rice, when used to produce *Niangao*, would cause marked changes in the amylose content and side chain length distribution of amylopectin in rice starch. These characteristics could improve the processing, texture profiles, and functional properties of *Niangao*, and ultimately the quality of *Niangao* products. Meanwhile, the WHC, moisture content, reducing sugar content, and color were also improved. In addition, fermentation enhanced the extensibility of *Niangao*, resulting in finer, smoother, and more delicious taste. Finally, fermentation inhibited the retrogradation of *Niangao* and enhanced the nutritional value of this food. Understanding the mechanism to prevent the retrogradation of *Niangao* at the molecular level would be useful in further kinetic studies.

5 Acknowledgements

The authors wish to acknowledge Doctoral Start-up Funding of Hubei University of Technology (No 4301/00047, BSQD2017016) and Nature Science Foundation of Hubei Province (4115/00051).

References

Alonso-Gomez, L., Niño-López, A. M., Romero-Garzón, A. M., Pineda-Gomez, P., & Real-Lopez, A. D. (2016). Physicochemical transformation of cassava starch during fermentation for production of sour starch in Colombia. *Stärke*, 68(11-12), 1139-1147. http://dx.doi.org/10.1002/star.201600059.

American Association of Cereal Chemist – AACC. (2000). *Method 44-15A, 46-11A, 08-01, and 30-10*. (10th ed.). St. Paul: AACC. Available in: <http://www.aaccnet.org/Pages/default.aspx>.

Auh, J. H., Chae, H. Y., Kim, Y. R., Shim, K. H., Yoo, S. H., & Park, K. H. (2006). Modification of rice starch by selective degradation of amylose using alkalophilic Bacillus cyclomaltodextrinase. *Journal of Agricultural and Food Chemistry*, 54(6), 2314-2319

Carmona-García, R., Bello-Pérez, L. A., Aguirre-Cruz, A., Aparicio-Saguilán, A., Hernández-Torres, J., & Alvarez-Ramirez, J. (2016). Effect of ultrasonic treatment on the morphological, physicochemical, functional, and rheological properties of starches with different granule size. *Stärke*, 68(9-10), 972-979. http://dx.doi.org/10.1002/star.201600019.

Dàvila, E., & Parés, D. (2007). Structure of heat-induced plasma protein gels studied by fractal and lacunarity analysis. *Food Hydrocolloids*, 21(2), 147-153. http://dx.doi.org/10.1016/j.foodhyd.2006.02.004.

Falguni, P., Sudhir, K. T., Yudhishthir, S. R., & Rameshwar, S. (2011). Characterization of mannitol producing strains of Leuconostoc species. *World Journal of Microbiology & Biotechnology*, 27(4), 933-939. http://dx.doi.org/10.1007/s11274-010-0536-y.

Franco, C. M., Cabral, R. A., & Tavares, D. Q. (2002). Structural and physicochemical characteristics of lintnerized native and sour cassava starches. *Stärke*, 54(10), 469-475. http://dx.doi.org/10.1002/1521-379X(200210)54:10<469::AID-STAR469>3.0.CO;2-Z.

Gunaratne, A., Sirisena, N., Ratnayaka, U. K., Ratnayaka, J., Kong, X., Vidhana Arachchi, L. P., & Corke, H. (2011). Effect of fertiliser on functional properties of flour from four rice varieties grown in Sri Lanka. *Journal of the Science of Food and Agriculture*, 91(7), 1271-1276. http://dx.doi.org/10.1002/jsfa.4310. PMid:21384369.

Hoove, R., & Vasanthan, T. (1993). The effect of annealing on the physicochemical properties of wheat, oat, potato and lentil starches. *Journal of Food Biochemistry*, 17(5), 303-325. http://dx.doi.org/10.1111/j.1745-4514.1993.tb00476.x.

Irondi, E. A., Awoyale, W., Oboh, G., & Boligon, A. A. (2017). Effect of mango kernel flour addition on the phenolics profile, antioxidant activity and pasting properties of wheat flour. *Journal of Food Measurement and Characterization*, 11(4), 2202-2210. http://dx.doi.org/10.1007/s11694-017-9605-3.

Jiang, X., Li, B., Su, Y., & Zhu, W. (2013). Shifts in bacterial community compositions during in vitro fermentation of Amylopectin and resistant starch by colonic inocula of pigs. *Journal of Food and Nutrition Research*, 1(6), 156-163. http://dx.doi.org/10.12691/jfnr-1-6-7.

Juliano, B. O., Tuaño, A. P. P., Monteroso, D. N., Aoki, N., Mestres, C., Duldulao, J. B. A., & Bergonio, K. B. (2012). Replacement of acetate with ammonium buffer to determine apparent amylose content of milled rice. *Cereal Foods World*, 57(1), 14-19. http://dx.doi.org/10.1094/CFW-57-1-0014.

Kancabaş, A., & Karakaya, S. (2013). Angiotensin-converting enzyme (ACE)-inhibitory activity of boza, a traditional fermented beverage. *Journal of the Science of Food and Agriculture*, 93(3), 641-645. http://dx.doi.org/10.1002/jsfa.5883. PMid:23001958.

Lu, Z. H., Li, L. T., Cao, W., Li, Z. G., & Tatsumi, E. (2003). Influence of natural fermentation on physico-chemical characteristics of rice noodles. *International Journal of Food Science & Technology*, 38(5), 505-510. http://dx.doi.org/10.1046/j.1365-2621.2003.00701.x.

Lu, Z. H., Li, L. T., Min, W. H., Wang, F., & Tatsumi, E. (2005). The effects of natural fermentation on the physical properties of rice flour and the rheological characteristics of rice noodles. *International Journal of Food Science & Technology*, 40(9), 985-992. http://dx.doi.org/10.1111/j.1365-2621.2005.01032.x.

Niu, H., Zhang, M. C., Xia, X. F., Liu, Q., & Kong, B. H. (2018). Effect of porcine plasma protein hydrolysates on long-term retrogradation of corn starch. *Food Chemistry*, 239, 172-179. http://dx.doi.org/10.1016/j.foodchem.2017.06.103. PMid:28873556.

Osella, C. A., Sánchez, H. D., Carrara, C. R., de la Torre, M. A., & Pilar Buera, M. (2005). Water redistribution and structural changes of starch during storage of a gluten-free bread. *Stärke*, 57(5), 208-216. http://dx.doi.org/10.1002/star.200400330.

Park, S. J., Ha, K. Y., & Shin, M. (2012). Properties and qualities of rice flours and gluten-free cupcakes made with higher-yield rice varieties in Korea. *Food Science and Biotechnology*, 21(2), 365-372. http://dx.doi.org/10.1007/s10068-012-0048-7.

Peng, H. L., Gan, Z. D., Xiong, H., Luo, M., Yu, N. X., Wen, T., Wang, R. H., & Li, Y. (2017). Self-Assembly of protein nanoparticles from rice bran waste and their use as delivery system for curcumin. *ACS Sustainable Chemistry & Engineering*, 5(8), 6605-6614. http://dx.doi.org/10.1021/acssuschemeng.7b00851.

Primo-Martin, C., Van Nieuwenhuijzen, N. H., Hamer, R. J., & Van Vliet, T. (2007). Crystallinity changes in wheat starch during the bread-making process: starch crystallinity in the bread crust. *Journal of Cereal Science*, 45(2), 219-226. http://dx.doi.org/10.1016/j.jcs.2006.08.009.

Qi, G. Y., & Sun, X. S. (2010). Soy protein adhesive blends with synthetic latex on wood veneer. *Journal of the American Oil Chemists' Society*, 88(2), 271-281. http://dx.doi.org/10.1007/s11746-010-1666-y.

Roman, L., Reguilon, M. P., & Gomez, M. (2017). Physicochemical characteristics of sauce model systems: Influence of particle size and extruded flour source. *Journal of Food Engineering*, 219, 93-100. http://dx.doi.org/10.1016/j.jfoodeng.2017.09.024.

Romano, A., Masi, P., Aversano, R., Carucci, F., Palomba, S., & Carputo, D. (2018). Microstructure and tuber properties of potato varieties with different genetic profiles. *Food Chemistry*, 239, 789-796. http://dx.doi.org/10.1016/j.foodchem.2017.07.010. PMid:28873636.

Santiago-Ramos, D., Figueroa-Cardenas, J. D., Veles-Medina, J. J., & Salazar, R. (2018). Physicochemical properties of nixtamalized black bean (Phaseolus vulgaris L.) flours. *Food Chemistry*, 240, 456-462. http://dx.doi.org/10.1016/j.foodchem.2017.07.156. PMid:28946298.

Seo, N. S., Roh, S. A., Auh, J. H., Park, J. H., Kim, Y. R., & Park, K. H. (2007). Structural characterization of rice starch in rice cake modified by thermus scotoductus 4-α-Glucanotransferase (TSαGTase). *Journal of Food Science*, 72(6), 331-336. http://dx.doi.org/10.1111/j.1750-3841.2007.00428.x. PMid:17995674.

Sharma, B., Gujral, H. S., & Solah, V. (2017). Effect of incorporating finger millet in wheat flour on mixolab behavior, chapatti quality and starch digestibility. *Food Chemistry*, 231, 156-164. http://dx.doi.org/10.1016/j.foodchem.2017.03.118. PMid:28449992.

Somsubsin, S., Seebunrueng, K., Boonchiangma, S., & Srijaranai, S. (2018). A simple solvent based microextraction for high performance liquid chromatographic analysis of aflatoxins in rice samples. *Talanta*, 176, 172-177. http://dx.doi.org/10.1016/j.talanta.2017.08.028. PMid:28917738.

Thiré, R. M., Simão, R. A., & Andrade, C. T. (2003). High resolution imaging of the microstructure of maize starch films. *Carbohydrate Polymers*, 54(2), 149-158. http://dx.doi.org/10.1016/S0144-8617(03)00167-X.

Vandeputte, G. E., Derycke, V., Geeroms, J., & Delcour, J. A. (2003). Rice starches. II. Structural aspects provide insight into swelling and pasting properties. *Journal of Cereal Science*, 38(1), 53-59. http://dx.doi.org/10.1016/S0733-5210(02)00141-8.

Wang, H., Liu, Y. F., Chen, L., Li, X. X., Wang, J., & Xie, F. W. (2018). Insights into the multi-scale structure and digestibility of heat-moisture treated rice starch. *Food Chemistry*, 242, 323-329. http://dx.doi.org/10.1016/j.foodchem.2017.09.014. PMid:29037696.

Wu, Y., Chen, Z., Li, X., & Wang, Z. (2010). Retrogradation properties of high amylose rice flour and rice starch by physical modification. *Lebensmittel-Wissenschaft + Technologie*, 43(3), 492-497. http://dx.doi.org/10.1016/j.lwt.2009.09.017.

Xie, L. H., Tang, S. Q., Luo, J., Wei, X. J., Shao, G. N., Jiao, G. A., Sheng, Z. H., & Hu, P. S. (2017). Physiochemical properties of rice starch for production of vermicelli with premium quality. *Journal of Food Science and Technology*, 54(12), 1-8. http://dx.doi.org/10.1007/s13197-017-2852-9. PMid:29085135.

Xiong, Y. Q., He, X. W., Zhang, E. J., & Huang, Q. (2010). The Preparation and Properties of Slowly Digestible Starch Produced by Recrystallization and Debranching. *Shipin Yu Fajiao Gongye*, 36(10), 42-45.

Yang, Y., & Tao, W. Y. (2008). Effects of lactic acid fermentation on FT-IR and pasting properties of rice flour. *Food Research International*, 41(9), 937-940. http://dx.doi.org/10.1016/j.foodres.2007.10.011.

Zhang, H., Feng, X., Larssen, T., Qiu, G., & Vogt, R. D. (2010). In inland China, rice, rather than fish, is the major pathway for methylmercury exposure. *Environmental Health Perspectives*, 118(9), 1183-1188. http://dx.doi.org/10.1289/ehp.1001915. PMid:20378486.

Zhou, W., Fang, R. S., & Chen, Q. H. (2017). Effect of gallic and protocatechuic acids on the metabolism of ethyl carbamate in Chinese yellow rice wine brewing. *Food Chemistry*, 233, 174-181. http://dx.doi.org/10.1016/j.foodchem.2017.04.113. PMid:28530563.

Zhu, F. (2018). Chemical composition and food uses of teff (Eragrostis tef). *Food Chemistry*, 239, 402-415. http://dx.doi.org/10.1016/j.foodchem.2017.06.101. PMid:28873585.